Title: Neuron-targeted caveolin-1 improves motor function and preserves memory in mice subjected to brain trauma

Junji Egawa#[1,2,5], Jan M. Schilling#[1,2], Weihua Cui#[1,2,6], Edmund Posadas[1,2], Atsushi Sawada[1,2], Basheer Alas[1,2], Alice E. Zemljic-Harpf[1,2], McKenzie Fallon[3,4], Chitra D. Mandyam[3,4], David M. Roth[1,2], Hemal H. Patel[1,2], Piyush M. Patel[1,2], Brian P. Head[1,2]†

[1]Veterans Affairs San Diego Healthcare System, 3350 La Jolla Village Drive, San Diego, CA 92161, USA

[2]Department of Anesthesiology, School of Medicine, University of California, San Diego, La Jolla, California 92093

[3]Skaggs School of Pharmacy and Pharmaceutical Sciences, University of California, San Diego, La Jolla, California 92093

[4]Committee on the Neurobiology of Addictive Disorders, The Scripps Research Institute, 10550 North Torrey Pines Road, SP30-2400, La Jolla, CA 92037

[5]Department of Anesthesiology, Nara Medical University, Kashihara, Japan

[6]Department of Anesthesiology, Beijing Tiantan Hospital, Capital Medical University, Beijing, China

#Drs. Egawa, Schilling and Cui share equal first authorship.

†Corresponding Author:

Brian P. Head, Department of Anesthesiology, University of California San Diego, VASDHS (9125), 3350 La Jolla Village Dr., San Diego, CA 92161, USA. E-mail: bhead@ucsd.edu

Abstract

BACKGROUND: Studies *in vitro* and *in vivo* demonstrate that membrane/lipid rafts (MLR) and caveolin (Cav) organize pro-growth receptors, and when over-expressed specifically in neurons, Cav-1 augments neuronal signaling and growth, and improves cognitive function in adult and aged mice. However, whether Cav-1 overexpression can preserve motor and cognitive function in the setting of brain trauma is unknown.

METHODS: Here, we engineered a neuron-targeted Cav-1 overexpressing transgenic (Tg) mouse (via synapsin promoter, SynCav1 Tg) and subjected it to a controlled cortical impact (CCI) model of brain trauma and measured biochemical, anatomical, and behavioral changes.

RESULTS: SynCav1 Tg mice exhibited increased hippocampal expression of Cav-1 and MLR-localization of PSD-95, NMDAR, and TrkB. When subjected to CCI, SynCav1 Tg mice demonstrated preserved hippocampal-dependent fear learning and memory, motor function recovery on inverted grid, and decreased brain lesion volume.

CONCLUSIONS: Neuron-targeted overexpression of Cav-1 in the adult brain preserves hippocampal-dependent learning and memory, restores motor function after brain trauma, and decreases brain lesion size. Our findings suggest neuron-targeted Cav-1 as a novel therapeutic strategy to restore nerve function and prevent trauma-associated neurodegeneration.

Introduction

Brain injury is a debilitating event that occurs when individuals are exposed to an external force that induces a focal and/or diffuse mechanical neuronal injury (axons and dendrites) and a damaged, growth-inhibitory environment resulting in chronic neurodegeneration. Individuals afflicted with various forms of nerve injury exhibit impaired motor and cognitive function, sensory loss, and chronic pain accompanied with poor functional recovery(1-4). The resultant nerve injury within the brain is a major contributing risk factor to neurodegenerative conditions such as Alzheimer's and Parkinson's disease (AD and PD), and amyotrophic lateral sclerosis (ALS)(1-6).

Nerve injury involves a biphasic progression(3, 7-9) consisting of an initial primary mechanical insult to neurons, followed by a secondary, delayed injury due to micro- and astrogliosis, and production of glial-derived myelin-associated growth inhibitors that limit neuroregenerative potential(10, 11). On a subcellular level, nerve injury decreases expression and subcellular localization of neuronal growth promoting receptors(12) and blunts production of downstream mediators of neuroplasticity(13, 14). This hostile environment limits the brain's regenerative capacity and ultimately leads to neurodegenerative disorders.

Genetic interventions that evoke intrinsic neuro-regenerative signaling cascades have the potential to restore functional network connectivity and improve functional recovery after nerve injury. Neuronal growth signaling pathways are dependent upon establishing a polarized plasma membrane and the localization of growth-promoting receptors to these polarized platforms(15). These platforms are composed of membrane lipid rafts (MLR), plasmalemmal microdomains enriched in sphingolipids, cholesterol, and scaffolding proteins known as caveolins (Cavs)(15). Within MLR, Cav-1 compartmentalizes key growth-promoting receptors in order to enhance 'high-fidelity' signal transduction(15-18). However, following nerve injury, the subcellular localization of these signaling components are significantly disorganized and/or decreased(12-14), which in part may explain for the inability of injury neurons to re-establish functional connections weeks to months after trauma.

We have previously shown that neuron-targeted overexpression of Cav-1 (achieved by linking it to a neuron-specific synapsin promoter [*SynCav1*]) enhances MLR formation, augments receptor-mediated cAMP production, TrkB signaling, and dendritic growth and arborization even in the presence of myelin-associated growth inhibitors(17). Moreover, *SynCav1* delivery to the hippocampus *in vivo* increased MLR and MLR-localized expression of TrkB, promoted structural and functional hippocampal neuroplasticity, and improved hippocampal-dependent learning and memory in aged mice(18), suggesting that genetic interventions that target MLR and Cav-1-associated microdomains may enhance the efficacy of existing pharmacologic agents or already present endogenous growth factors to improve neuronal function after nerve injury or in the neurodegenerative brain.

The present study tested whether neuron-targeted over-expression of Cav-1 can protect neurons

against brain trauma and improve behavioral recovery. To achieve this, we engineered a SynCav1 transgenic mouse (SynCav1 Tg) and subjected it to a controlled cortical impact (CCI) model of brain trauma model(12). Akin to our results with the *SynCav1* gene construct *in vitro* and *in vivo*(17, 18), biochemical characterization of SynCav1 Tg mice demonstrated higher Cav-1 expression and increased MLR-localization of synaptic components (e.g., PSD95, NMDAR and TrkB). Two months following CCI, SynCav1 Tg mice exhibited preserved hippocampal-dependent fear learning and memory, better motor function recovery, and smaller brain lesion when compared to Tg negative (Tg neg). These results are the first to demonstrate that global neuron-targeted overexpression of Cav-1 preserves and/or restores cognitive and motor function after brain trauma, and extend previous work from our group that neuron-targeted Cav-1 may be exploited as a potential therapeutic target for promoting functional neurooplasticity after trauma or in certain neurodegenerative conditions such as AD, PD, and ALS.

METHODS and MATERIALS

Animals

All mice (C57BL/6; Jackson Laboratories) were treated in compliance with the Guide for the Care and Use of Laboratory Animals (National Academy of Science, Washington, D.C.). All animal use protocols were approved by the Veterans Administration San Diego Healthcare System Institutional Animal Care and Use Committee (IACUC, San Diego, California) prior to procedures performed. Male adult (4 month) mice were housed under normal conditions with *ad libitum* access to food and water. Two weeks after behavior testing all mice were euthanized with 50 mg/kg pentobarbital and brain tissue was processed for histology and measurement of lesion size as previously described(12). SynCav1 transgenic (SynCav1 Tg) mice were generated in C57BL/6 background through the UCSD mouse transgenic core(19). Full length Cav-1 cDNA (537 bp) was cloned into a vector containing the human neuron-specific synapsin promoter (495 bp)(20) and termed SynCav1 as previously described(17, 18). SynCav1 DNA construct (free of ethidium bromide) was used for microinjection (UCSD Transgenic Core). Transgene negative (Tg neg) and SynCav1 transgene positive (SynCav1 Tg) mice were used for this study. Mice were allocated to 4 groups: Sham Tg neg, TBI Tg neg, Sham SynCav1 Tg, and TBI SynCav1 Tg.

Genotyping

SynCav1 transgene (SynCav1) positive mice were confirmed by tail DNA extraction and polymerase chain reaction (PCR). Briefly, genomic DNA was extracted from tail tissue samples using the Qiagen DNeasy Blood and Tissue Kit (# 69504). PCR was performed for *SynCav1* genes using the following protocol: denaturation at 95°C for 5 minutes, followed by 30 cycles at 95°C for 30 seconds, 58.5°C for 30 seconds, and 72°C for 45 seconds, and then 72°C for 7 minutes and hold at 4°C. All of the primers are purchased from Integrated DNA Technologies and shipped in lyophilized form. The oligonucleotide primer sequences are as follows: SynCav1 *Forward* [5'-CAG CTT CAG CAC CGC GGA CA-3' (#138389038)] and SynCav1 *Reverse* [CAC CTC GTC TGC CAT GGC CT-3' (#138389039)] were used to detect a product size of 470 bp (Figure 1A lower bands). For genotyping control, vinculin *Forward* [Ex3 823F: 5'-CCT GCG CGG GAT TAC CTC ATT GAC-3' (#138389036)] and vinculin *Reverse* [Ex4 1642R: 5'-TGC TCA CCT GGC CCA AGA TTC TTT-3' (#138389037)] were used to detect a product size of 860 bp. PCR products were separated on a 1 % agarose gel and run for 35 minutes at 135 volts.

Biochemical Characterization of Membrane/Lipid Rafts (MLR)

Sucrose density fraction of mouse brains were performed as previously described(12, 17, 18). Mice were sacrificed by rapid decapitation under isoflurane (5%) anesthesia. The whole brain was quickly removed and hippocampal tissue (bilateral, CA regions and dentate gyrus combined, 50-100 mg) was dissected and homogenized using a carbonate lysis buffer (500 mM sodium carbonate, pH 11.0) containing protease and phosphatase inhibitors. Protein was quantified by Bradford assay and normalized to 0.5 mg/ml. Sucrose density gradients were prepared as previously reported. Membranes samples (f4-5 and f10-12) were incubated overnight with primary antibodies for Cav-1 (Cell Signaling #3238, 1:1000), β_3-tubulin (Abcam ab18207, 1:1000), TrkB (BD Biosciences 610102, 1:1000), or NMDAR2A (abcam ab124913, 1:750), NMDAR2B (abcam ab28373, 1:750), or PSD95 and probed with species-specific secondary antibodies conjugated to HRP. Densitometric analysis (arbitrary units) was conducted as previously described(12, 17, 18).

Controlled Cortical Impact (CCI) Model

Mice were fixed into a stereotactic frame under isoflurane anesthesia (5% induction for 30 sec followed by 1.5% maintenance mixed with oxygen at 1 liter/min). A portable drill was used to perform a craniotomy over the right hemisphere to generate a burr hole exposing a portion of the primary and secondary motor cortex and parietal-temporal cortex (+1 to − 4 A-P from the bregmatic suture and 4 mm laterally from the sagittal suture), a modification of our previously publishes work with the CCI model(12). The bone flap was carefully removed and a 3 mm diameter piston was centered on dura at approximately +0.5 to -2.5 mm bregma and 3 mm lateral to the saggital suture. Using a stereotaxic impactor (Impact OneTM; myNeuroLab.com), the 3 mm diameter piston was accelerated at a speed of 5 m/second; the depth of the impact was 1 mm below the cortical surface. Animals were placed on a 37°C warm water blanket to until they awoke post-surgery.

Histology and Lesion Volume Analysis

To measure the lesion volume, animals were transcardially perfused with 4% paraformaldehyde in 0.1 M PO_4 buffer 2 months post-CCI. After perfusion, samples were stored in the same buffer for 24 hours and processed for histology. Serial coronal hippocampal sections (100 μm serial sections) were stained with Cresyl Violet (Abcam). Sections were mounted on superfrost slides, dried overnight and processed for citric acid treatment(21). After cooling with 1xPBS sections were incubated with Cresyl Violet for 15 minutes at RT and washed with 1xPBS 3x. Following washes sections were dehydrated with ethanol and cleared with citrasolv and coverslipped with DPX (electron microscopy sciences). To image the entire coronal sections from +4.2 to -5.6 bregma, 15-25 pictures were obtained at 10X on a BZ9000 Imager (Keyence Osaka, Japan) and were combined using the image stitching function of the BZ-X Analyzer software. For quantitation of lesion volume, digital virtual slides obtained with Aperio Scanscope CS-1 scanner were used for extensive computer assisted morphometry in a Spectrum image analysis system (Aperio Technology Inc., 1700 Leider Lane, Buffalo Grove, IL, 60089, USA) followed by Scanscope software and associated algorithm analysis as previously described(12, 22).

Inverted Grid Test

We performed the inverted grid at baseline, and weekly intervals starting at day 7 up to day 49 post impact to measure basic motor function in our animals. The inverted grid test measures the mouse's ability to voluntarily hang on an inverted wire mesh(23). The apparatus is elevated 40 cm above the ground with a soft surface underneath to prevent physical trauma to the mice. Latency to fall measurements were repeated 3-times with an inter-trial interval of 30 seconds (sec). The holding impulse was then calculated by multiplying the longest hanging duration of the three trials by the mouse's body weight [time (sec.) * body weight (g)].

Fear Conditioning Behavior

Fear conditioning was performed as previously described(18). Foot shocks were delivered through the floor consisting of 36 stainless steel rods wired to a shock generator. Presentation of unconditioned stimuli (US: scrambled foot shock) and conditioned stimuli (CS: auditory tone) were controlled by computer (Med Associates Inc.). Freezing was determined using analysis software (Video Freeze®, Med Associates Inc., ANY-MAZE, San Diego Instruments). Training: After an acclimation period (2 min), mice were presented with a tone (CS: 90 dB, 5 kHz) for 30s that co-terminated with a foot shock (US: 2.0s, 1.0 mA) in dark chambers. A total of three tone-shock pairings were presented with a varying inter-trial interval of 30-90s. Freezing was measured during each CS to measure fear acquisition level across groups. Context fear was tested twenty-four hours later. Cued fear was tested twenty-four hours after context fear. To remove contextual cues, the chambers were altered across several dimensions (odor - scent; visual – light chambers and walls are altered via plastic inserts; tactile – smooth plastic floor covering) to minimize generalization from the conditioning context. The session started with a 3 min acclimation period, during which time no tones were presented ("pre-tone" period), then 10 blocks of 5 CSs were presented for 30s each with an inter-trial interval of 5s. Freezing was recorded during each CS presentation. For analysis, total freezing was averaged as total freezing during all CS presentations.

Statistical Analyses

Data were checked for normal distribution and then analyzed with 2-way repeated measure ANOVA, 2-way ANOVA, or student's t-test. Following, unpaired *t*-tests and Fisher's LSD post hoc comparison were performed as appropriate. For the analysis we used IBM SPSS v22 and GraphPad Prism 6 (La Jolla, CA). Data are presented as mean ± SEM. Significance was assumed when $p < 0.05$. Experimental groups were blinded to the experimenters and code was broken only for analysis as previously described(18).

RESULTS

Synapsin-Caveolin-1 Transgenic (SynCav1 TG) Mice have more MLR and MLR-Associated Synaptic Receptors

SynCav1 TG positive mice were confirmed by polymerase chain reaction (PCR) and ethidium bromide DNA gel electrophoresis (Figure 1). SynCav1 appears at 470 bp as indicated by the white arrow on left side of DNA molecular ladder. Vinculin (upper band) was used as a loading control (860 bp). To assess whether SynCav1 Tg positive mice exhibited changes in MLR-associated proteins, sucrose density fractionation was performed on hippocampal (*Hpc*) homogenates from negative and positive TG mice followed by immunoblot blot assay and analysis. *Hpc* homogenates from SynCav1 TG positive mice showed a significant (n = 3-4 mice/group; TG negative vs. SynCav1 TG positive, respectively) increase in Cav-1 [0.39 ± 0.03 vs 0.79 ± 0.02; ($t(6) = 10.55$, $p < 0.001$)], PSD95 [0.55 ± 0.03 vs 0.88 ± 0.04; ($t(6) = 6.27$, $p < 0.001$)], NMDAR2A (NR2A) [0.78 ± 0.02 vs 2.18 ± 0.32; ($t(5) = 3.77$, $p = 0.01$)], NR2B [0.52 ± 0.04 vs 1.50 vs 0.09; ($t(4) = 9.99$, $p = 0.0006$)], and TrkB [0.73 ± 0.22 vs 1.94 ± 0.16; ($t(5) = 4.55$, $p = 0.006$)] protein expression compared to Hpc from TG negative mice (Figure 2A & 2B). Sucrose density fractionation revealed a significant increase in Cav-1 [11061 ± 1740 vs 20517 ± 2550; ($t(4) = 3.06$, $p = 0.04$)], PSD95 [8423 ± 907 vs 24587 vs 2408; ($t(4) = 6.28$, $p = 0.003$)], NR2A [9859 ± 511 vs 13951 ± 212; ($t(4) = 7.39$, $p = 0.002$)], NR2B [9308 ± 900 vs 17685 ± 2200; ($t(4) = 3.52$, $p = 0.02$)], and TrkB [12944 ± 1064 vs 18183 ± 1659; ($t(6) = 2.66$, $p = 0.04$)] in buoyant fractions 4 and 5 (MLR fractions) indicating an increased in MLR-associated synaptic proteins (Figure 2B & 2C).

SynCav1 TG Mice Exhibit Improved Motor Function Recovery after Brain Trauma

We have previously shown that TBI decreases MLR and MLR-associated synaptic protein complexes(12), all of which are important for neuroprotection(16), neuronal signaling and plasticity(17), and neurobehavior(18). As evident in Figure 2, because SynCav1 Tg mice expressed more MLR and MLR-localized synaptic proteins necessary for neuroprotective signaling, we therefore tested whether these mice exhibited a neuroprotective phenotype following TBI. To analyze motor function using the Inverted Grid, we performed a 2-way Repeated Measure ANOVA with 'gene' and 'TBI' as the between subject factor (n = 11 – 22 mice/group). The Inverted Grid test revealed a significant effect of time (Greenhouse-Geisser correction: F (2.4,164.5) = 10.61, $p < 0.001$) and time * TBI (Greenhouse-Geisser correction: F (2.4,164.5) = 5.58, p = 0.003) for the recovery period between 7 and 49 days post injury, while the time * strain (Greenhouse-Geisser correction: F (2.4,164.5) = 0.81, p = 0.47) or time * TBI * strain interaction (Greenhouse-Geisser correction: F (2.4,164.5) = 1.02, p = 0.37) was not significantly different between groups. No significant baseline difference before injury between groups was observed. We then assessed recovery from injury over time by comparing, within each group, the change from the first (day 7) to the last (day 49) day post TBI or sham surgery. Interestingly all groups, except for the Tg neg subjected to TBI, significantly increased their holding impulse over this time period as assessed by a paired t-test (Figure 3). Specifically, the Holding Impulse [body weight (g) * hanging time (sec.)/10^2] was increased between day 7 and day 49 for sham-Tg neg [34.1 ± 6.1 vs 67.0 ± 13.8; (t(20) = -3.28, p = 0.004)], sham-SynCav1 [37.0 ± 7.4 vs 87.1 ± 17.6; (t(10) = -3.51, p = 0.006)], and TBI-SynCav1 [20.4 ± 3.1 vs 33.0 ± 5.1; (t(21) = -3.00, p = 0.007)], respectively. This was not the case for TBI-Tg neg mice [17.0 ± 3.0 vs 21.7 ± 3.4; (t(19) = -1.86, p = 0.08)]. These results demonstrate that 7 weeks after being subjected to TBI, SynCav1 TG positive, but not Tg negative mice, exhibited motor function recovery.

SynCav1 TG Mice Show Preserved Contextual Fear Memory and Smaller Lesion Size after Brain Trauma

We have previously shown that *SynCav1* gene delivery to the brain improves hippocampal-dependent learning and memory in adult and aged mice(18). Therefore, in the present model we wanted to assess

hippocampal function in our SynCav1 transgenic mouse after TBI (Figure 4). A 2-way Repeated Measure ANOVA with 'gene' and 'TBI' as the between subject factor was performed for percent freezing during the learning phase on day 1. Fear conditioning revealed no learning difference between groups (n = 21-22 mice/group) during the acquisition period, represented by no significant effect of 'time * gene * TBI' (Huynh-Feldt correction: F (1.67,145.66) = 0.18, p = 0.80) (Figure 4A). In all groups, similar increases in freezing over time with repeated CS-US pairing trials were apparent (Huynh-Feldt correction: F (1.67,145.66) = 196.26, $p < 0.001$). On day 2, contextual re-exposure was performed to assess hippocampal-dependent learning and memory. The 2-Way ANOVA revealed a trending ($p < 0.1$) interaction for 'TBI * strain' F (1,82) = 3.066, p = 0.08) with decreased % freezing in Tg neg mice subjected to TBI (Figure 3b, black bars), with no significant main factor effect for 'TBI' F (1,82) = 1.81, p = 0.18) or 'strain' F (1,82) = 1.96, p = 0.17). In contrast, SynCav1 Tg mice subjected to TBI TBI exhibited a similar % freezing to that observed in Tg neg sham mice [post hoc Fisher's LSD comparison between Tg neg/Sham (40.0 ± 3.65 % Freezing) and Tg neg/TBI (29.72 ± 2.03) (t(82) = 2.17, p = 0.03), as well as Tg neg/TBI (29.72 ± 2.03) and SynCav1/TBI (40.19 ± 2.69) (t(82) = 2.23, p = 0.03)], thus demonstrating preserved or improved hippocampal-dependent learning and memory SynCav1 Tg mice after TBI (Figure 4B); no significant difference between groups was observed in the cued re-exposure on day 3 (Figure 4C). After completion of the behavioral testing, we performed histological analysis using Cresyl violet stain to measure brain lesion volume from rostral to caudal as described in the *Methods* section. Figure 5 represents histological brain (n = 4 mice/group) sections showing damage to the motor cortex at bregma -0.50 mm (Figure 5A) and damage to the parietal cortex and underlying dorsal hippocampus at bregma -2.70 (Figure 5B). Postmortem analysis revealed that CCI significantly increase brain lesion volume in TG negative mice (6.9 ± 1.0 mm^3; F(1,12) = 46.68, $p < 0.0001$; Figure 5C) compared to sham TG negative mice (craniotomy only; 0.005 ± 0.003 mm^3). In contrast, CCI-induced brain lesion volume was significantly reduced in SynCav1 TG positive mice (1.7 ± 0.7 mm^3; F(1,12) = 17.64, p = 0.001, n=4) compared to TG negative mice subjected to CCI. These findings may in part explain for the motor and hippocampal-dependent behavioral resilience exhibited by SynCav1 TG mice subjected to CCI show in Figures 3 and 4.

Discussion

Although previous work shows that increasing Cav-1 and MLRs specifically in neurons is neuroprotective(16), enhances pro-growth signaling, promotes neuroplasticity(17), and improves learning and memory in aged mice(18), the functional significance of neuron-targeted Cav-1 in the setting of brain trauma is not kown. In this study, we demonstrate that a mouse genetically engineered to contain a neuron-targeted Cav-1 construct expresses more MLR-associated synaptic proteins (PSD-95) and receptors (NR2A, NR2B, TrkB), exhibits greater motor function recovery, and demonstrates preserved contextual learning and memory months following brain trauma. This study provides proof of concept results that neuron-targeted over-expression of Cav-1 is neuroprotective against brain injury and extends upon previous findings that Cav-1 plays a necessary role in neurobehavioral function.

Brain trauma disrupts neuronal networks and deteriorates cognitive function(3). The primary impact consists of mechanical-focal damage, diffuse axonal injury, and subsequent neuronal cell loss. The secondary delayed injury increases neuroinflammation, production of pro-inflammatory and growth inhibitory cytokines such as IL-1β, TNFα, and IFNγ(12, 24), all of which lead to chronic micro- and astrogliosis, and production of myelin-associated growth inhibitors (MAIs) such as myelin-associated glycoproteins (MAG) and Nogo that contribute to the delayed secondary injury(11). Secondary injury occurs hours to days to months after the initial primary impact and results in neurochemical, metabolic and cellular changes. The hostile environment generated by the activated microglia triggers the recruitment and chronic activation of astrocytes (i.e., astrogiosis). Astrogliosis is characterized by cellular proliferation and hypertrophy as demarked by increased glial fibrillary acidic protein expression, an intermediate filament protein. We have previously shown in our CCI model, cortical (motor and parietal) and hippocampal damage, neuronal and neuropil loss, disruption of MLR and MLR-associated neuroprotective signaling components such as NMDARs and TrkB, and a significant increase in growth inhibitory cytokines and chemokines(12). In the present study, the severe motor cortical damaged was evident relatively early as indicated by measurable functional motor deficits as assessed in the inverted grid test (Figure 3). However, when subjected to CCI, the SynCav1 Tg mice demonstrated better motor

function recovery over time, demonstrating greater resilience when compared to Tg neg. The dorsal hippocampus which lies directly under the parietal cortex, was also severely injured as demonstrated by decreased hippocampal-dependent contextual fear learning and memory (Figure 4) and hippocampal tissue loss (Figure 5). Similar to the motor recovery, SynCav1 TG mice also demonstrated preserved hippocampal-dependent contextual fear learning and memory. We have previously shown that *SynCav1* gene delivery significantly promotes dendritic growth and arborization in primary neurons even in the presence of growth inhibitory cytokines and MAI(17), neuroprotective results which could explain in part for the observed improvement in both motor and hippocampal-dependent memory function exhibited by SynCav1 Tg mice in the present study. Although the current study used well-established behavioral tests to assess changes in motor and memory, more sensitive electrophysiological assays such as motor evoke potentials (MEPs) and/or excitatory post-synaptic potentials (EPSP) would yield a better understanding of which neuronal circuits are disrupted in the current brain trauma model as well as which neuronal circuits are preserved in the SynCav1 Tg mouse.

Restoration of functional neuronal connectivity is in part dependent upon establishing a polarized plasma membrane and the localization of functional pro-growth signaling receptors to these polarized platforms, thus transducing extracellular growth-stimulating cues to the underlying dynamic cytoskeleton(15, 25). These pro-growth signaling pathways promote axonal transport, dendritic growth, and formation of synaptic contacts. However, after nerve injury, the subcellular localization of these signaling components become disorganized or are decreased(12-14). A critical component of neuronal cell membrane polarity are MLR(15, 26), cholesterol and lipid enriched microdomains within the plasma membrane that partition synaptic proteins involved in signaling and plasticity(27). Cav-1 along with MLR provide this polarized membrane-signaling platform that facilitates intrinsic neuronal growth and repair, maintenance and neuroplasticity(15, 25). The importance of MLR in proper neuronal growth signaling, synaptic maintenance and neuroplasticity is underscored by evidence that disruption of MLR leads to synaptic loss, reduced dendritic spines, receptor instability, and disrupted growth cone motility(26, 27). Evidence shows that exogenous application of the pro-growth neurotrophin brain-derived neurotrophic factor (BDNF) enhances cholesterol in neurons and raises levels of neuronal Cav-1(28); moreover

BDNF-TrkB signaling is dependent upon TrkB recruitment into neuronal MLR(29). The present study shows that SynCav1 Tg mice have enhanced TrkB expression in MLR (Figure 2), a subcellular event which not only facilitates BDNF-TrkB signaling, but is also critical for other tyrosine kinase receptor signaling cascades(27) and could contribute to the neurobehavioral resilience exhibited by the SynCav1 Tg mice following brain trauma.

Individuals with brain injury have an increased risk of neurological complications, neuropathological and neuropsychiatric changes, deficits in attention, suffer from post-traumatic stress disorder (PTSD), and have a higher incidence of neurodegenerative diseases such as AD, PD, and ALS later in life(6, 30-33). Disabilities associated with nerve injury lead to a greater requirement for institutional and long-term care in addition to exacerbating the already existing domestic burden, which bares with it an emotional, psychological, and physical cost. Despite intense investigative efforts, there is a lack of defined therapeutic approaches for the treatment of nerve injury, predominantly because many targeted therapies are often ineffective in eliciting the desired response, likely due to decreased expression of key receptors (TrkB, GPCRs)(12) and blunted second messenger (cAMP) signaling cascades necessary to evoke functional neuroplasticity(13, 14, 34). These pro-growth signaling deficits limit the capacity for neuroregeneration and re-innervation of neuronal circuits to their appropriate targets. Therefore, there exists an urgent need for the development of more innovative methods to limit neurodegeneration and improve neurologic function post injury. The delayed nature of the secondary injury suggests a potential therapeutic window to prevent progressive neurodegeneration by re-evoking neuroplastic signaling mechanisms, enhancing neuroregenerative capacity, and improving motor and cognitive function after injury. Therefore, genetic interventions like neuron-targeted Cav-1, which not only enhances pro-growth/survival signaling within neurons and improves learning and memory, may also be exploited as a potential therapy to not only reverse complications associated with brain trauma, but might also protected against spinal cord trauma.

Certain approaches such as the use of biologics (stem cells, peptide and gene therapy, exogenous growth factors), pharmacological agents, and/or noninvasive interventions (exercise or transcranial magnetic stimulation (TMS)) may work synergistically to improve motor and cognitive function months to

years post brain trauma(24, 35). For example, *SynCav1*, which enhances MLR formation, receptor-mediated cAMP production, and TrkB signaling in neurons, could be used in combination with selective pharmacologic agents that stimulate MLR-associated TrkB receptors(36), augment cAMP with phophodiesterase inhibitors(13, 34, 37), or increase serotonin and/or dopamine with selective reuptake inhibitors(38-40) to promote functional neuroplasticity and improve behavior. In addition, non-invasive interventions such as exercise therapy or TMS can augment production of pro-growth molecules such as BDNF(35) and activate TrkB signaling(41). Thus enhancing TrkB-localization to MLR with neuron-targeted Cav-1 may work in concert with these non-invasive interventions to evoke neuroplastic changes necessary to improve motor and neurobehavioral function in individuals afflicted with brain trauma and trauma-induced neurodegeneration.

Conflict of Interest

The work was supported by grant from the Department of Veterans Affairs BX001225 (BPH), BX000783 (DMR) and BX001963 (HHP), and National Institutes of Health NS073653 (BPH), HL091071 (HHP), HL107200 (HHP and DMR), HL066941 (HHP and DMR), HL115933 (HHP and DMR), MH094151 and MH019934 (DVJ) and DA034140 (C. D. Mandyam). The authors declare no conflicting financial interest.

REFERENCES

1. Lew HL, Garvert DW, Pogoda TK, Hsu PT, Devine JM, White DK, et al. (2009): Auditory and visual impairments in patients with blast-related traumatic brain injury: Effect of dual sensory impairment on Functional Independence Measure. *J Rehabil Res Dev*. 46:819-826.

2. Lew HL, Otis JD, Tun C, Kerns RD, Clark ME, Cifu DX (2009): Prevalence of chronic pain, posttraumatic stress disorder, and persistent postconcussive symptoms in OIF/OEF veterans: polytrauma clinical triad. *J Rehabil Res Dev*. 46:697-702.

3. Sharp DJ, Scott G, Leech R (2014): Network dysfunction after traumatic brain injury. *Nature reviews Neurology*. 10:156-166.

4. King PR, Beehler GP, Wade MJ (2015): Self-Reported Pain and Pain Management Strategies

Among Veterans With Traumatic Brain Injury: A Pilot Study. *Mil Med*. 180:863-868.

5. Goldstein LE, Fisher AM, Tagge CA, Zhang XL, Velisek L, Sullivan JA, et al. (2012): Chronic traumatic encephalopathy in blast-exposed military veterans and a blast neurotrauma mouse model. *Science translational medicine*. 4:134ra160.

6. Vincent AS, Roebuck-Spencer TM, Cernich A (2014): Cognitive changes and dementia risk after traumatic brain injury: implications for aging military personnel. *Alzheimers Dement*. 10:S174-187.

7. Das M, Mohapatra S, Mohapatra SS (2012): New perspectives on central and peripheral immune responses to acute traumatic brain injury. *Journal of neuroinflammation*. 9:236.

8. Kumar A, Loane DJ (2012): Neuroinflammation after traumatic brain injury: opportunities for therapeutic intervention. *Brain, behavior, and immunity*. 26:1191-1201.

9. DeKosky ST, Blennow K, Ikonomovic MD, Gandy S (2013): Acute and chronic traumatic encephalopathies: pathogenesis and biomarkers. *Nature reviews Neurology*. 9:192-200.

10. Israelsson C, Flygt J, Astrand E, Kiwanuka O, Bengtsson H, Marklund N (2014): Altered expression of myelin-associated inhibitors and their receptors after traumatic brain injury in the mouse. *Restor Neurol Neurosci*. 32:717-731.

11. Schwab ME, Strittmatter SM (2014): Nogo limits neural plasticity and recovery from injury. *Curr Opin Neurobiol*. 27:53-60.

12. Niesman IR, Schilling JM, Shapiro LA, Kellerhals SE, Bonds JA, Kleschevnikov AM, et al. (2014): Traumatic brain injury enhances neuroinflammation and lesion volume in caveolin deficient mice. *Journal of neuroinflammation*. 11:39.

13. Atkins CM, Oliva AA, Jr., Alonso OF, Pearse DD, Bramlett HM, Dietrich WD (2007): Modulation of the cAMP signaling pathway after traumatic brain injury. *Experimental neurology*. 208:145-158.

14. Atkins CM, Falo MC, Alonso OF, Bramlett HM, Dietrich WD (2009): Deficits in ERK and CREB activation in the hippocampus after traumatic brain injury. *Neuroscience letters*. 459:52-56.

15. Head BP, Patel HH, Insel PA (2013): Interaction of membrane/lipid rafts with the cytoskeleton: Impact on signaling and function: Membrane/lipid rafts, mediators of cytoskeletal arrangement and cell signaling. *Biochimica et biophysica acta*.

16. Head BP, Patel HH, Tsutsumi YM, Hu Y, Mejia T, Mora RC, et al. (2008): Caveolin-1 expression is essential for N-methyl-D-aspartate receptor-mediated Src and extracellular signal-regulated kinase 1/2 activation and protection of primary neurons from ischemic cell death. *Faseb J*. 22:828-840.

17. Head BP, Hu Y, Finley JC, Saldana MD, Bonds JA, Miyanohara A, et al. (2011): Neuron-targeted caveolin-1 protein enhances signaling and promotes arborization of primary neurons. *The Journal of biological chemistry*. 286:33310-33321.

18. Mandyam CD, Schilling JM, Cui W, Egawa J, Niesman IR, Kellerhals SE, et al. (2015): Neuron-Targeted Caveolin-1 Improves Molecular Signaling, Plasticity, and Behavior Dependent on the Hippocampus in Adult and Aged Mice. *Biol Psychiatry*.

19. Tsutsumi YM, Horikawa YT, Jennings MM, Kidd MW, Niesman IR, Yokoyama U, et al. (2008): Cardiac-specific overexpression of caveolin-3 induces endogenous cardiac protection by mimicking ischemic preconditioning. *Circulation*. 118:1979-1988.

20. Glover CP, Bienemann AS, Heywood DJ, Cosgrave AS, Uney JB (2002): Adenoviral-mediated, high-level, cell-specific transgene expression: a SYN1-WPRE cassette mediates increased transgene expression with no loss of neuron specificity. *Mol Ther*. 5:509-516.

21. Mandyam CD, Norris RD, Eisch AJ (2004): Chronic morphine induces premature mitosis of proliferating cells in the adult mouse subgranular zone. *J Neurosci Res*. 76:783-794.

22. Krajewska M, You Z, Rong J, Kress C, Huang X, Yang J, et al. (2011): Neuronal deletion of caspase 8 protects against brain injury in mouse models of controlled cortical impact and kainic acid-induced excitotoxicity. *PloS one*. 6:e24341.

23. Carlson CG, Rutter J, Bledsoe C, Singh R, Hoff H, Bruemmer K, et al. (2010): A simple protocol for assessing inter-trial and inter-examiner reliability for two noninvasive measures of limb muscle strength. *Journal of neuroscience methods*. 186:226-230.

24. Pearn ML, Niesman IR, Egawa J, Sawada A, Almenar-Queralt A, Shah SB, et al. (2016): Pathophysiology Associated with Traumatic Brain Injury: Current Treatments and Potential Novel Therapeutics. *Cell Mol Neurobiol*.

25. Egawa J, Pearn ML, Lemkuil BP, Patel PM, Head BP (2016): Membrane lipid rafts and

neurobiology: age-related changes in membrane lipids and loss of neuronal function. *J Physiol*. 594:4565-4579.

26. Guirland C, Zheng JQ (2007): Membrane lipid rafts and their role in axon guidance. *Adv Exp Med Biol*. 621:144-155.

27. Zonta B, Minichiello L (2013): Synaptic membrane rafts: traffic lights for local neurotrophin signaling? *Frontiers in synaptic neuroscience*. 5:9.

28. Suzuki S, Kiyosue K, Hazama S, Ogura A, Kashihara M, Hara T, et al. (2007): Brain-derived neurotrophic factor regulates cholesterol metabolism for synapse development. *J Neurosci*. 27:6417-6427.

29. Suzuki S, Numakawa T, Shimazu K, Koshimizu H, Hara T, Hatanaka H, et al. (2004): BDNF-induced recruitment of TrkB receptor into neuronal lipid rafts: roles in synaptic modulation. *J Cell Biol*. 167:1205-1215.

30. Fleminger S, Oliver DL, Lovestone S, Rabe-Hesketh S, Giora A (2003): Head injury as a risk factor for Alzheimer's disease: the evidence 10 years on; a partial replication. *Journal of neurology, neurosurgery, and psychiatry*. 74:857-862.

31. Medicine Io (2006): *Amyotrophic Lateral Sclerosis in Veterans: Review of the Scientific Literature*. Washington, DC: The National Academies Press.

32. Sharp DJ (2014): The association of traumatic brain injury with rate of progression of cognitive and functional impairment in a population-based cohort of Alzheimer's disease: the Cache County dementia progression study by Gilbert et al. Late effects of traumatic brain injury on dementia progression. *International psychogeriatrics / IPA*. 26:1591-1592.

33. Chapman JC, Diaz-Arrastia R (2014): Military traumatic brain injury: a review. *Alzheimers Dement*. 10:S97-104.

34. Atkins CM, Cepero ML, Kang Y, Liebl DJ, Dietrich WD (2013): Effects of early rolipram treatment on histopathological outcome after controlled cortical impact injury in mice. *Neuroscience letters*. 532:1-6.

35. Cramer SC, Sur M, Dobkin BH, O'Brien C, Sanger TD, Trojanowski JQ, et al. (2011): Harnessing neuroplasticity for clinical applications. *Brain : a journal of neurology*. 134:1591-1609.

36. English AW, Liu K, Nicolini JM, Mulligan AM, Ye K (2013): Small-molecule trkB agonists promote axon regeneration in cut peripheral nerves. *Proceedings of the National Academy of Sciences of the United States of America*. 110:16217-16222.

37. Titus DJ, Sakurai A, Kang Y, Furones C, Jergova S, Santos R, et al. (2013): Phosphodiesterase inhibition rescues chronic cognitive deficits induced by traumatic brain injury. *J Neurosci*. 33:5216-5226.

38. Ma M, Li L, Wang X, Bull DL, Shofer FS, Meaney DF, et al. (2012): Short-duration treatment with the calpain inhibitor MDL-28170 does not protect axonal transport in an in vivo model of traumatic axonal injury. *Journal of neurotrauma*. 29:445-451.

39. Kaminska K, Golembiowska K, Rogoz Z (2013): Effect of risperidone on the fluoxetine-induced changes in extracellular dopamine, serotonin and noradrenaline in the rat frontal cortex. *Pharmacological reports : PR*. 65:1144-1151.

40. Huot P, Johnston TH, Lewis KD, Koprich JB, Reyes MG, Fox SH, et al. (2014): UWA-121, a mixed dopamine and serotonin re-uptake inhibitor, enhances l-DOPA anti-parkinsonian action without worsening dyskinesia or psychosis-like behaviours in the MPTP-lesioned common marmoset. *Neuropharmacology*.

41. Ma J, Zhang Z, Su Y, Kang L, Geng D, Wang Y, et al. (2013): Magnetic stimulation modulates structural synaptic plasticity and regulates BDNF-TrkB signal pathway in cultured hippocampal neurons. *Neurochemistry international*. 62:84-91.

FIGURES

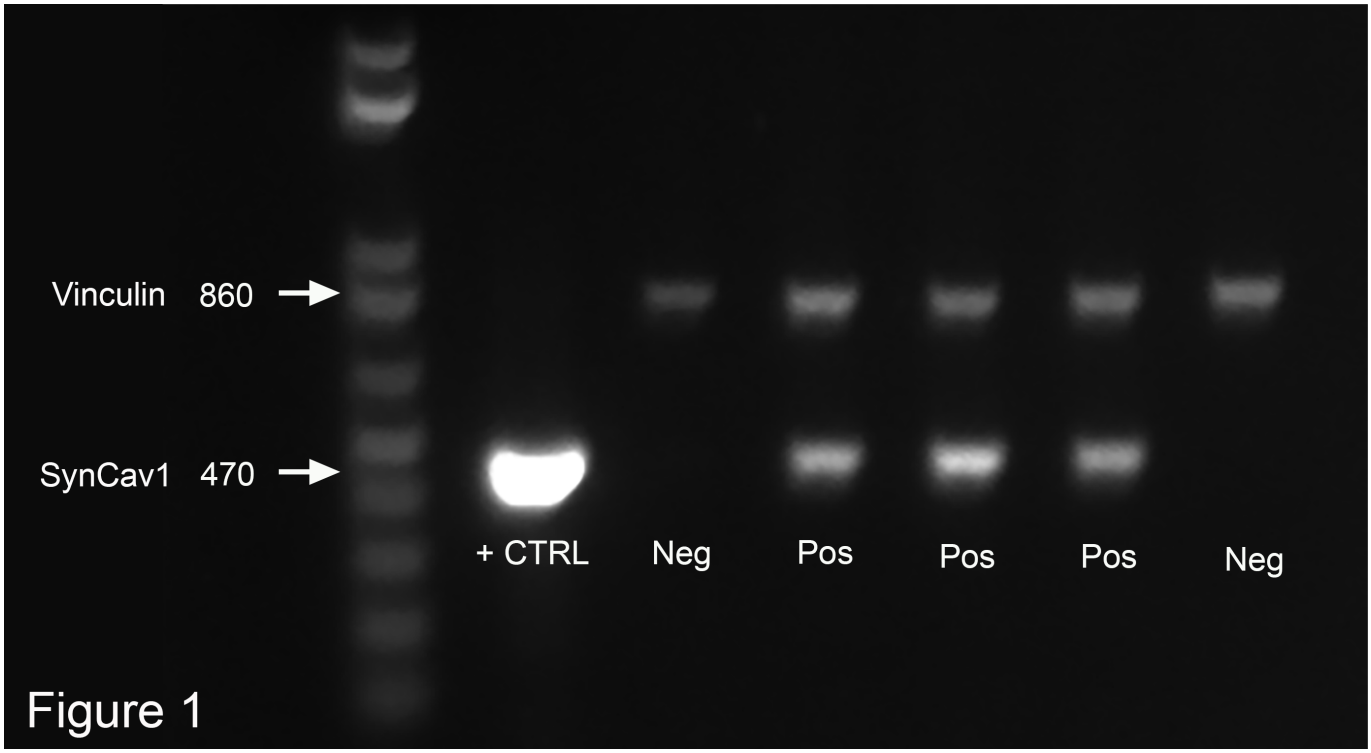

Figure 1. SynCav1 TG positive mice were confirmed by polymerase chain reaction (PCR) and ethidium bromide DNA gel electrophoresis. SynCav1 appears at 470 base pairs (bp) as indicated by the white arrow on left side of DNA molecular ladder. Vinculin (upper band) was used as a loading control (860 bp).

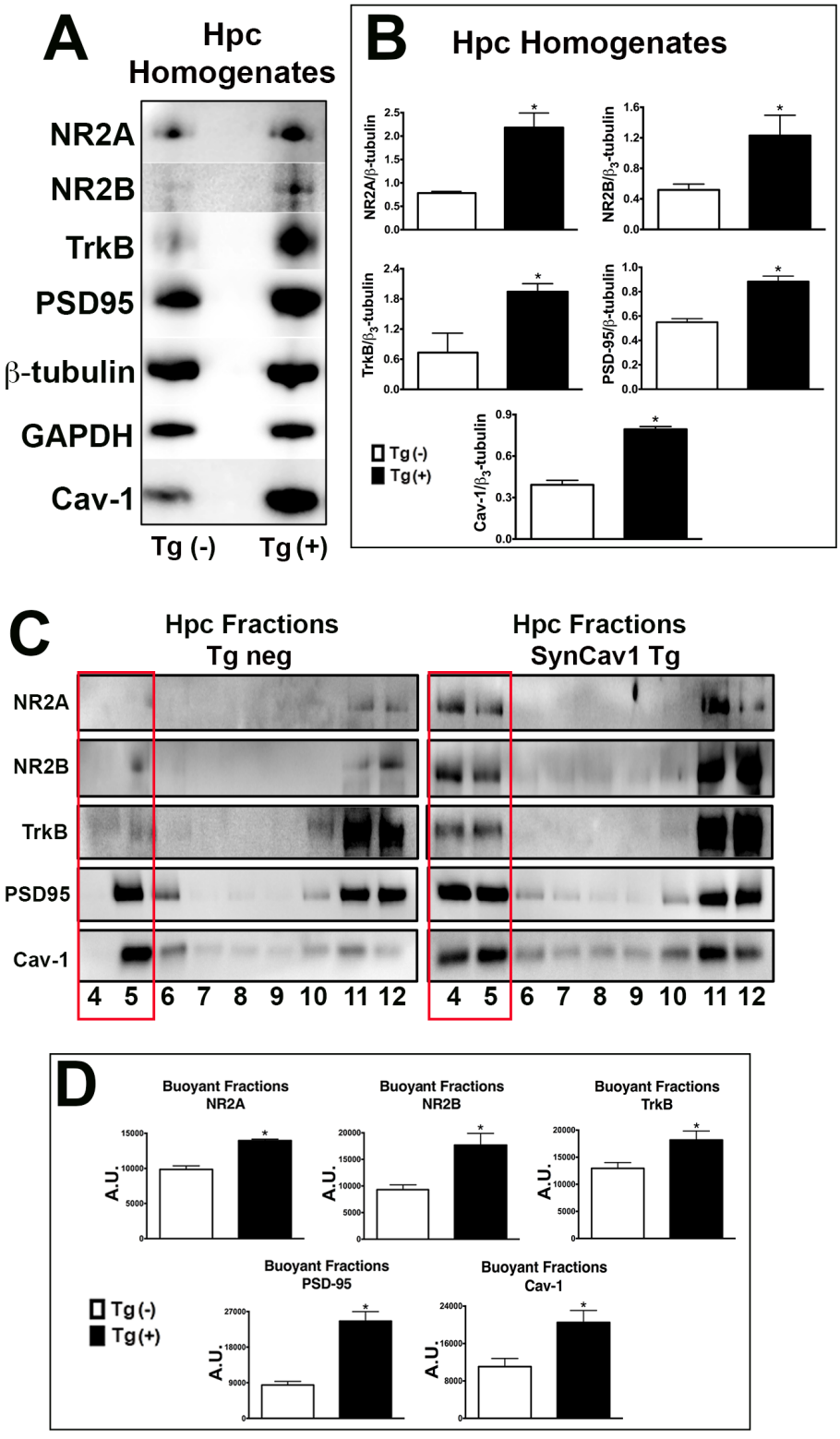

Figure 2

Figure 2. SynCav1 Tg mice express more hippocampal MLR-localized NMDARs (NRs), TrkB, and Cav-1. Hippocampal (*Hpc*) homogenates from Tg neg and SynCav1 Tg mice were immunoblotted for Cav-1, PSD95, NMDAR2A (NR2A), NR2B, and TrkB (**A**). β_3-tubulin and glyceraldehyde 3-phosphate

dehydrogenase (GAPDH) were used as loading controls. Quantitation of protein expression are shown in **B**. Hpc tissue were subjected to sucrose density fractionation followed by immunoblot analysis for Cav-1, PSD95, NR2A, NR2B, and TrkB (**C**). Quantitation of protein expression are shown in **D**. Tg neg, open box; SynCav1 Tg, black box. All fractions were generated from equal protein loading of 0.5 mg/ml. Data (*n* = 3-4 mice/group) represent arbitrary units (A.U.) mean SEM. Significance was assumed when *$p < 0.05$.

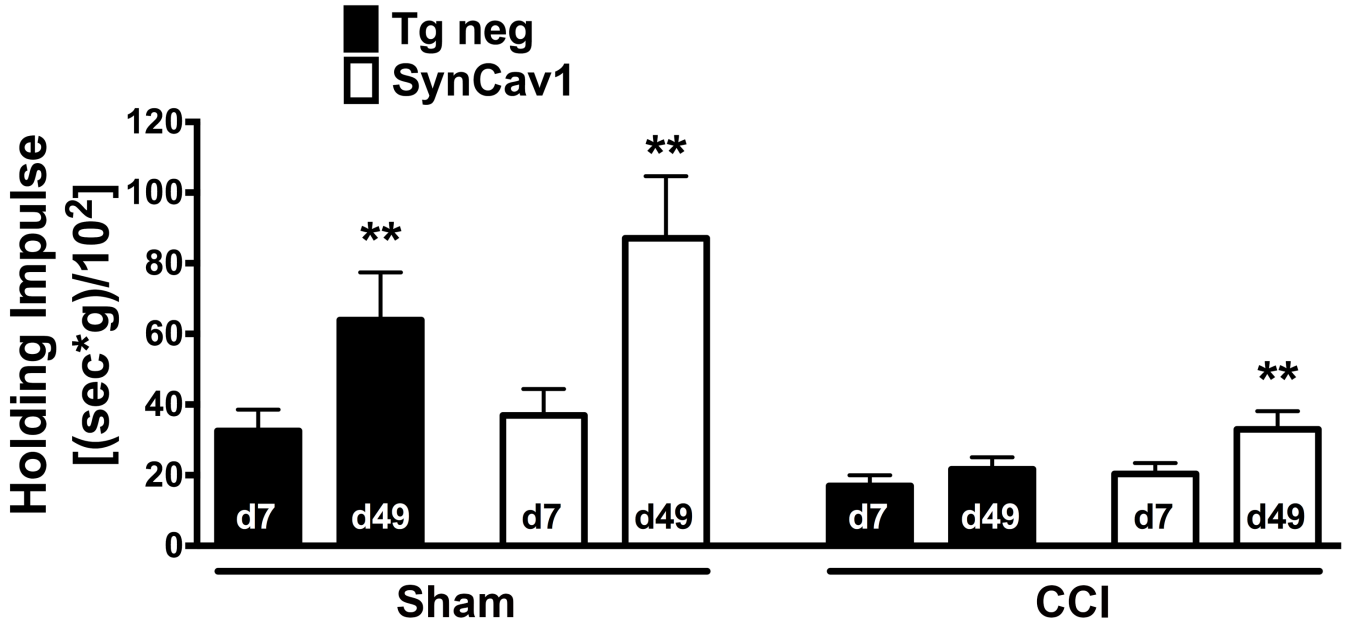

Figure 3

Figure 3. SynCav1 TG Mice Exhibit Improved Motor Function Recovery after Brain Trauma. TBI resulted in a significant decrease in holding impulse in both Tg neg (black bars) and SynCav1 mice (open bars) on day 7. When comparing the recovery between day 7 and day 49 with a paired t-test, all groups except for TBI/sham significantly improved their motor recovery as indicated by a significant increase in the holding impulse [body weight (g) * hanging time (sec.)/10^2]. Data (*n* = 11-22 mice/group) are presented as mean ± SEM. Significance was assumed when **$p < 0.05$.

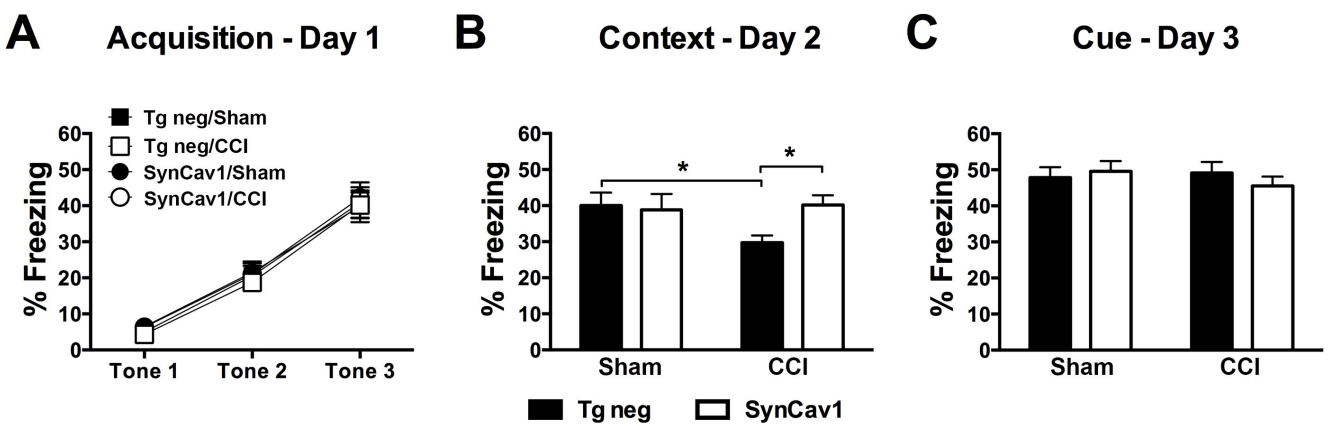

Figure 4

Figure 4. SynCav1 TG mice show preserved contextual fear learning and memory months after brain trauma. (**A**) Both groups showed similar acquisition in response to the conditioned stimulus 2 months post CCI; this was reflected in a significant effect of time during the repetitive exposure of the tone/shock pairings, with no significance for gene or time x gene interaction. (**B**) On day 2, contextual re-exposure demonstrated a significant decrease in percent freezing in Tg neg/TBI mice (black bars) (*p = 0.03) versus Tg neg/Sham. SynCav1/TBI mice (open bars) demonstrated significant preserved or improved hippocampal-dependent learning and memory (*p = 0.03) when compared to Tg neg/TBI mice. (**C**) No significant difference between groups was observed in the cued re-exposure on day 3. Data (n = 21-22 mice/group) are presented as mean ± SEM. Significance was assumed when $p < 0.05$.

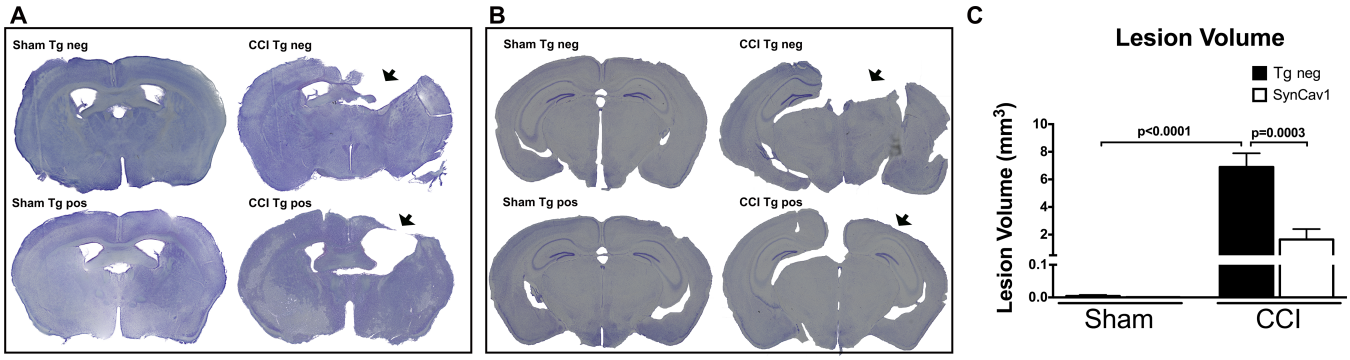

Figure 5

Figure 5. SynCav1 TG mice exhibit smaller cortical lesion size 2 months after brain trauma. Bright field microscopy of Cresyl violet stained brain sections showing damage to the motor cortex at bregma -0.50 mm (**A**) and damage to the parietal cortex and underlying dorsal hippocampus at bregma -2.70 (**B**). Quantitation of total lesion volume (mm^3) is shown in **C**. Data (n = 4 mice/group) are presented as mean ±

SEM. Significance was assumed when $p < 0.05$.